Chinese Science Bulletin 2005 Vol. 50 No. 24 2804—2808

Microstructure and mechanical properties of a novel Zr-based bulk metallic glass composite

SUN Yufeng[1,2], WANG Yuren[1], GUO Jian[3], WEI Bingchen[1] & LI Weihuo[1]

1. National Microgravity Lab, Institute of Mechanics, Chinese Academy of Sciences, Beijing 100080, China;
2. Research Central for Materials, Department of Materials Science and Engineering, Zhengzhou University, Zhengzhou 450002, China;
3. Department of Materials and Chemical Engineering, Zhongyuan Institute of Technology, Zhengzhou 450002, China

Correspondence should be addressed to Wang Yuren (email: wangyr@imech.ac.cn)

Abstract **$Zr_{48.5}Cu_{46.5}Al_5$ bulk metallic glass (BMG) composites with diameters of 3 and 4 mm were prepared through suction casting in an arc melting furnace by modulating the alloy composition around the monothetic BMG composition of the high glass forming ability. Microstructural characterization reveals that the composites contain micron-sized CuZr phase with martensite structure, as well as nano-sized Zr_2Cu crystalline particles and $Cu_{10}Zr_7$ plate-like phase embedded in an amorphous matrix. Room temperature compression tests showed that the composites exhibited significant strain hardening and obvious plastic strain of 7.7% for 3 mm and 6.4% for 4 mm diameter samples, respectively.**

Keywords: bulk metallic glass; composites, shear bands, plastic deformation, microstructure.

DOI: 10.1360/982004-856

Compared with the conventional crystalline materials, bulk metallic glass with the long range atomic disorder was regarded as a very promising structural material for their unique properties, such as high yield strength, high hardness, excellent corrosion and wear resistances. However, most of the BMGs exhibit inhomogeneous plastic deformation under quasistatic loading at room temperature. The plastic deformation of the BMGs is highly localized within a single or a few shear bands, which leads to instantaneous catastrophic shear failure after maximum yielding. Under tension test, the BMGs undergo drastic fracture after yielding and have no global plasticity. Even under compression test, the BMGs present no more than 2% plastic deformation after reaching its elastic limit. As a consequence, the brittleness of BMGs greatly limited their applications as engineering materials[1−6]. In order to improve the BMGs plastic deformation ability, an effective way was to produce BMG matrix composites. The reinforcement phase in the BMG composites can successfully restrict the nucleation and propagation of the highly localized shear bands and is helpful for the multiplication of shear bands. Therefore, the BMG composites could endure more plastic deformation than the monothetic BMGs[7−11]. Recently, BMG composites have been developed by utilizing a variety of crystalline reinforcements, such as refractory metals, ceramic particles, carbon or metal fibres. In particular, Hays et al.[12] were the first to develop a Zr-Ti-Cu-Ni-Be BMG composite containing b.c.c ductile dendritic β solid solution as a toughening phase by adding Nb to the alloy melt. The composite exhibits remarkably improved plastic deformation and obvious strain hardening on the premise of preserving its high fracture strength. Shortly after this, Kűhn and He et al.[13−15] fabricated Be-free Zr and Ti-based ductile dendrite reinforced BMG composites by introducing Nb or Ta refractory metals into the alloys since dislocation motion, twining and phase transformation induced plasticity are expected to be brought about by these ductile phases. Martensite phases, which contain numerous defects, have been used as reinforcement in many fields to improve the ductility or toughness of the materials, such as austenitic steel and ceramics. On the other hand, strain hardening of the materials can also be attributed to the stress-induced matensite phase transformation under deformation. However, no BMG matrix composite containing martensite phase has been developed as yet.

Newly discovered Cu-Zr-Al ternary alloys were reported to have high glass forming ability. According to the Cu-Zr-Al ternary phase diagram, CuZr intermetallic compound can be precipitated from the glass matrix in a certain alloy composition range[16]. CuZr with 1∶1 atomic ratio is a well-known martensite phase and can be formed at a high cooling rate. In this research, we developed a novel $Zr_{48.5}Cu_{46.5}Al_5$ ternary BMG composite by modulating the alloy composition around the BMG composition of the high glass forming ability. It contains strip-like martensite phase. The composites have not only high ultimate fracture strength, but also apparent strain hardening and significant plastic deformation before failure under uniaxial compression at room temperature.

1 Experimental

A master alloy with nominal composition of $Zr_{48.5}Cu_{46.5}Al_5$ was prepared by arc melting under a Ti-gettered argon atmosphere. From this master alloy, bulk alloy rods with 3 and 4 mm diameters and 70 mm length were prepared by suction cast into a water-cooled copper mold in a purified argon atmosphere. Slices cut from the alloy rods were used for thermal stability analysis. The thermal stability analysis was performed by a Perkin Elmer DSC-7 calorimeter in a flowing argon atmosphere (heating rate 20 $K \cdot min^{-1}$). The phase constitution was analyzed by SIMENS 500 X-ray diffraction (XRD). Scanning electron microscopy (JSEM 5520) and transmission electron mi-

croscopy (Philips TECNAI 20) were used for the microstructure analysis. TEM samples were electropolished using a solution mixture at the ratio of $HF:HClO_4:CH_4O = 1:1:9$. Room temperature compression tests were carried out with an Instron 5562 testing device under quasi-static loading (initial strain rate of $1\times10^{-4}\ s^{-1}$).

2 Results and discussion

Fig. 1 shows the XRD patterns from the central and the peripheral region of the as-cast composites. It can be seen that different phases were obtained in the different regions due to the local cooling rate variation. Only a broad amorphous diffraction peak can be recognized for the peripheral regions for all kinds of samples, which indicated that the peripheral regions have monothetic amorphous structures. In contrast, crystalline diffraction peaks superimposed on the broad amorphous diffraction peak could be well recognized in the XRD patterns taken from the central regions. The analysis shows that 3mm sample contained CuZr crystallinephase, while 4-mm sample were composed of $Cu_{10}Zr_7$ and Zr_2Cu phases.

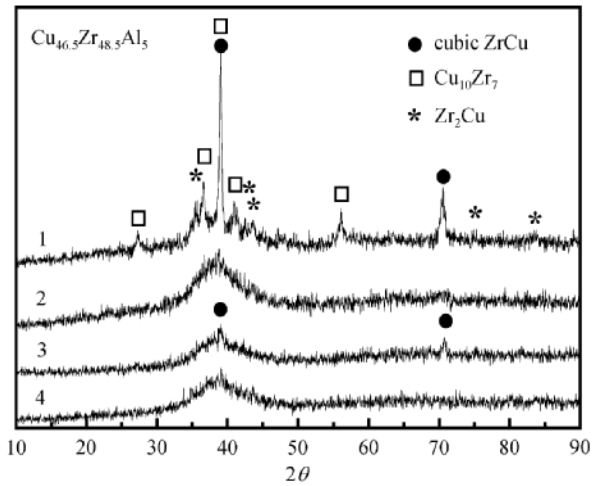

Fig. 1. XRD patterns taken from different parts of the composites. 1, Central region; 2, peripheral region of ϕ 4 mm alloy rods; 3, central region; 4, peripheral region of ϕ 3 mm alloy rods.

Fig. 2 shows the DSC scans of the as-cast $Zr_{48.5}Cu_{46.5}Al_5$ composites with the diameters of 3 mm and 4 mm, respectively. From the DSC curve, both of samples undergo an obvious glass transition T_g followed by one exothermic reaction T_x. T_g and T_x for ϕ3 mm and ϕ4 mm samples are 689, 741, 683 and 734 K, respectively. Therefore, the undercooled liquid regions for the two samples are nearly the same, 52 K for 3-mm diameter sample and 51 K for 4-mm diameter sample, respectively. However, the crystallization reaction heat of 3-mm sample is higher than that of 4-mm sample, which reveals that the 4-mm sample contains more crystalline phase than 3-mm sample.

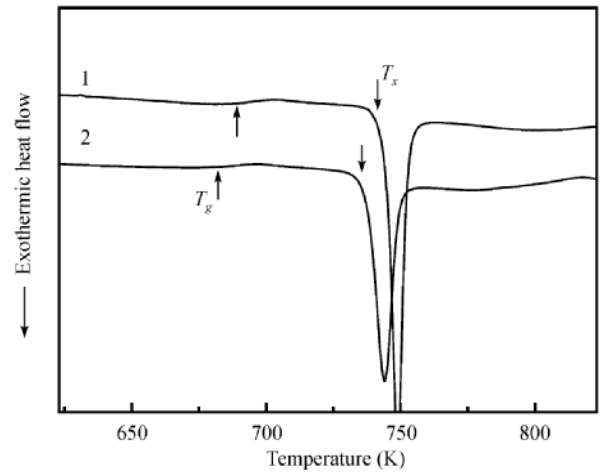

Fig. 2. DSC curves of the as-cast $Zr_{48.5}Cu_{46.5}Al_5$ composites with the diameters of 1/ ϕ3 mm; and 2/ ϕ4 mm.

Further microstructural analysis demonstrated that there is a microstructural transition from the peripheral region to the central region. As a typical example, Fig. 3(a) presents the SEM image of the 4-mm sample. No crystalline domain can be observed in the peripheral region, while blocky grains and grain boundary can be clearly identified in the central region. Fig. 3(b) shows the SEM image of the blocky grains in a large magnitude. The size of the blocky grain is about 50 μm. The surface morphology of the grain is irregular and some subgrains can be observed in the blocky grain, which reveals that martensite phase transformation might occur during the sample preparation process.

TEM analysis of the as-cast composites reveals that the peripheral region contains homogeneously amorphous phase for both of 3-mm and 4-mm samples. However, the microstructure feature in the central region is quite different. Some of the grains are CuZr intermetallic compound containing strip-like martensite phase, while others contain precipitated crystals embedded in the amorphous matrix. The microstructure of the central part of the samples 4 mm in diameter is depicted in Fig. 4. Fig. 4(a) shows the CuZr grains containing martensite structure. The SAED pattern inset in Fig. 4(a) was taken along the [311] zone axial, indicating that the parent phase is a B2 CuZr phase (CsCl type) with a lattice constant of a=3.256 Å. Previous study on the microstructure of CuZr compound has proved that CuZr is a martensite phase. Numerous defects from micro- to macro-twins can be observed in all samples of CuZr phase, regardless of the preparation technique. The CuZr martensite phase has a very complex superstructure. The interface between basic and superstructure regions is often but not always parallel with the microtwin planes[17−20]. Fig. 4(b) shows the TEM image in a high magnification, indicating that the martensite phase consists of a large amount of stacking faults. Fig. 4(c) shows the amor-

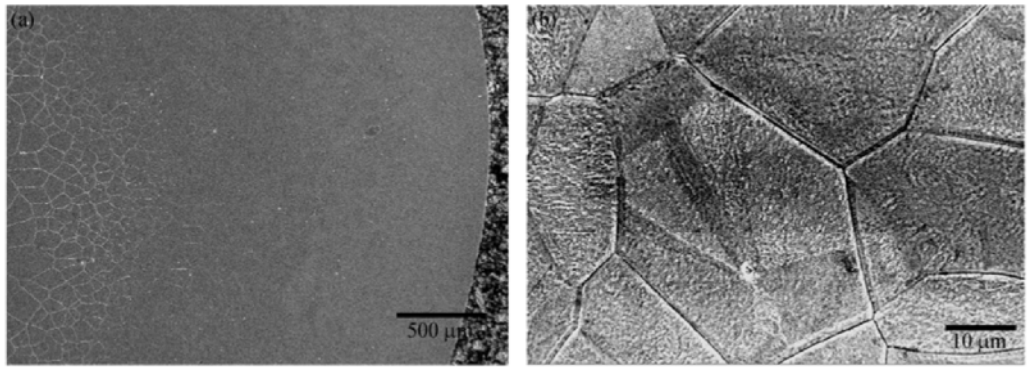

Fig. 3. (a) SEM image showing the microstructure transition of the as-cast 4 mm diameter composites; (b) SEM image of the internal microstructure of the blocky grains.

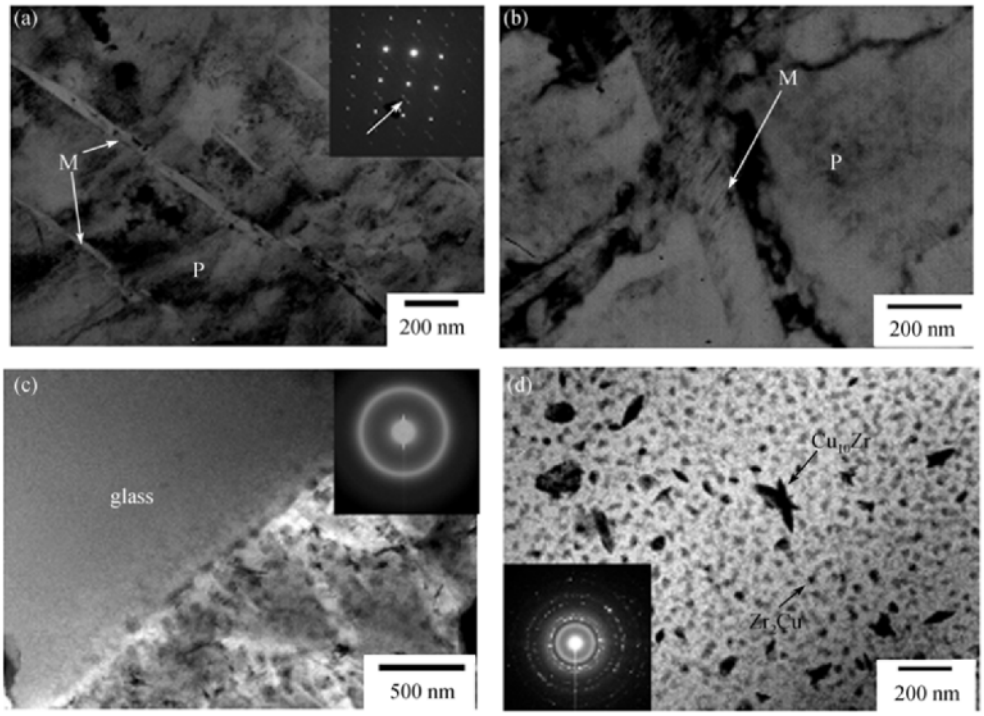

Fig. 4. TEM image showing the microstructure of the grains in the central part of the as-cast samples. (a) and (b) CuZr intermetallic compound containing martensite phase, "M" for martenstie phase and "P" for parent phase; (c) and (d) nanocrystalline Zr_2Cu particles and plate-like $Cu_{10}Zr_7$ phase embedded in amorphous matrix.

phous phase and the crystalline precipitates distributed in the amorphous matrix. An obvious boundary between the two regions can be seen. Fig. 4(d) shows the microstructure of the nanocrystal/glass matrix. The precipitated crystals can be assigned to the mixture of nano-sized Zr_2Cu particles and plate-like $Cu_{10}Zr_7$ phase according to its SAED pattern shown at the bottom panel[21]. For 3- mm diameter sample, nanocrystalline Zr_2Cu phase and plate-like $Cu_{10}Zr_7$ phase can also be found, but its volume fraction is too small to be detected by XRD measurement.

From the above description, it is concluded that the microstructure depends strongly on the local cooling rate and the alloy composition during the solidification process. The alloy melts will freeze into an amorphous phase in the peripheral region where the sample has a relatively high cooling rate close to the water-cooled copper mold. In contrast, a relatively low cooling rate in the centralal part of the sample induced the precipitation of the CuZr phase and martensite phase transformation. With the formation of the CuZr phase, the residual melt is lacking Cu and Zr elements. This results in an excess of Al element in the residual melt. The composition deviation of the melt facilitated glass formation. Therefore, the amorphous structure could be found in the central region. However, the

CuZr phase is unstable. Some of CuZr phase in the region of a relatively low cooling rate might decompose into $Cu_{10}Zr_7$ and Zr_2Cu phases during the final stage of alloy solidification.

A series of room temperature compression tests under quasistatic loading were carried out. The compression stress-strain curves for 3-mm and 4-mm diameter samples are shown in Fig.5. It shows that the two samples have undergone obvious strain hardening and plastic deformation prior to failure. For 3-mm diameter sample, the ultimate fracture strength is 1894 MPa, with a yield strength of 1332 MPa and plastic strain of 7.7%. For 4-mm diameter sample, the ultimate fracture strength is 1910 MPa, with a yield strength of 1624 MPa and plastic deformation of 6.4%.

The room temperature compression tests suggested that the deformation of $Zr_{48.5}Cu_{46.5}Al_5$ composites was induced by the formation and propagation of multiple shear bands in the shear plane, which is inclined at an angle of about 45° to the loading direction. The morphology of the lateral surface of the 4-mm diameter sample after compression test was shown in Fig. 6(a). Multiple shear bands indicated by the arrows can be observed near the fracture plane. Fig. 6(b) shows the fracture plane and the loading direction in the central part of the samples, which is viewed in the direction perpendicular to the fracture plane.

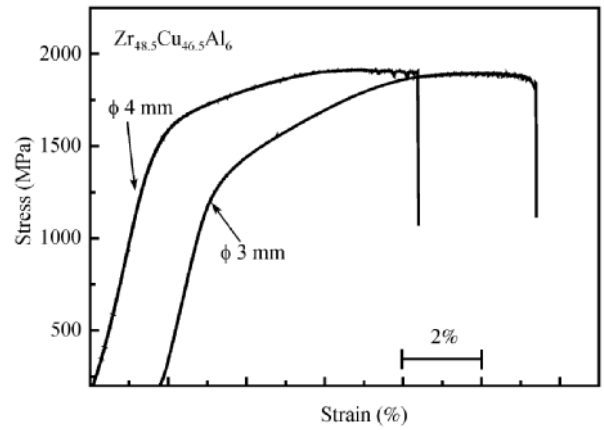

Fig. 5. Room temperature compression stress-strain curves for as-cast $Zr_{48.5}Cu_{46.5}Al_5$ composites.

Grains bent perpendicular to the loading direction indicated that a large plastic deformation occurred. The viscous flow traces and molten area can be clearly observed due to the adiabatic temperature elevation of the amorphous matrix. Fig. 6(c) shows the morphology of the peripheral part of the fracture plane. Typical vein patterns originated from the shearing-off and ripping apart of the shear bands can be found. The vein patterns in this case

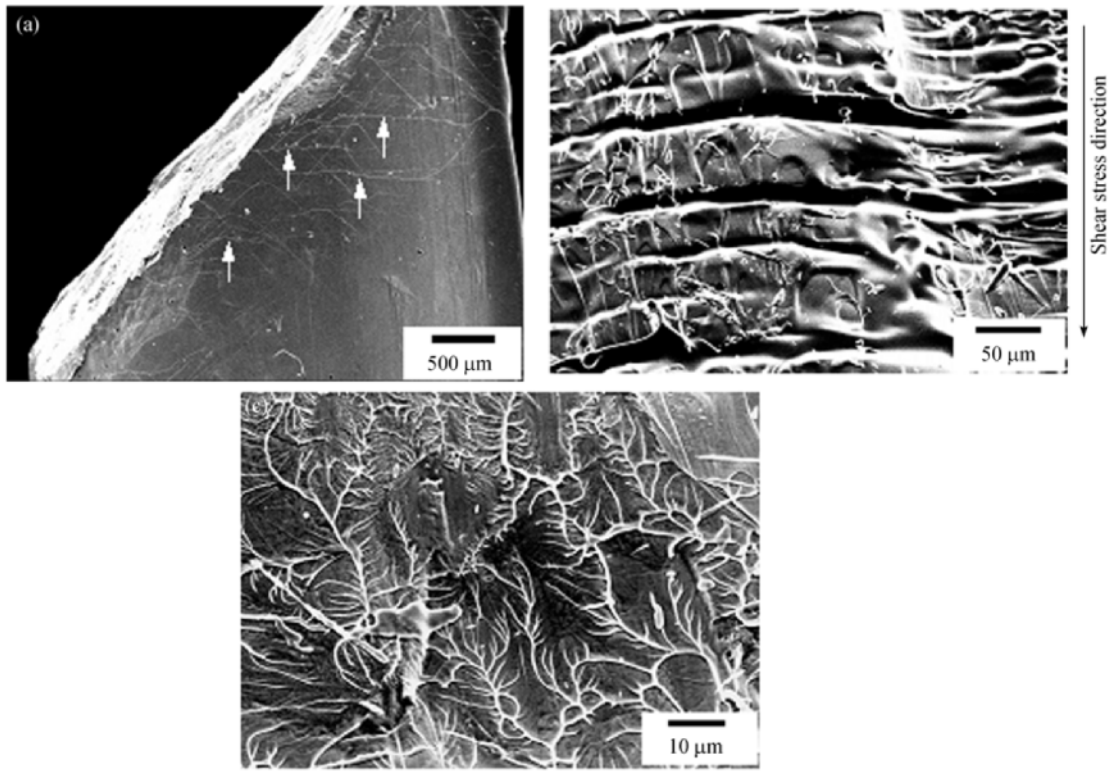

Fig. 6. SEM image showing the morphology of the fracture plane from 4 mm diameter composite. (a) Global profile near the fracture plane; (b) central part of the fracture plane; (c) peripheral part of the fracture plane.

are more branched and interlaced than the vein patterns of fractured monolithic BMG.

Generally speaking, deformation of monothetic BMG always concentrated in one or a few shear bands, while the other shear bands have little deformation. After yielding, the sample will experience work-softening. This finally leads to catastrophic failure without obvious plastic strain. It is also believed that the nanocrystals embedded in the amorphous matrix can only enhance strength, but cannot induce strain hardening due to the lack of numerous dislocations. The presence of $Cu_{10}Zr_7$ plate-like phase is deleterious to the improvement of the mechanical properties because $Cu_{10}Zr_7$ is a brittle intermetallic compound. In the present experiment condition, one of the factors that can promote the strain hardening, we believe, is the twinning deformation in the micrometer-sized b.c.c CuZr grains. The formation of the martensite phase leads to the generation of large density of twins and dislocations. Upon loading, the load transfers from the amorphous matrix to the CuZr intermetallic compound. The CuZr will undergo large strain hardening and plastic deformation by the twining deformation and more martensite phase is expected to be transformed. It is worthy noting that, although the distribution of crystalline phase is centralized in the central part of the sample, the nanocrystalline phase and the CuZr phase do hinder the propagation of the shear bands throughout the whole sample. In consequence, they promote the formation of multiple shear bands. The interaction among the crystals and the shear bands can also be confirmed by the branched shear bands pattern in the lateral surface and the vein patterns in the fracture plane.

3 Conclusions

In conclusion, the $Zr_{48.5}Cu_{46.5}Al_5$ BMG composites can be synthesized by modulating the alloy composition around that of high glass forming ability. The BMG composites contain ductile martensite phase, nano-sized particles and plate-like phase embedded in the amorphous matrix. The plastic deformation of the composites is enhanced by restricting the propagation of highly localized shear bands under loading. The CuZr grains are bent perpendicular to the loading direction, resulting in plastic strain of about 7.7% and 6.4% for 3- mm and 4-mm diameter samples respectively. These results show that we can obtain novel BMG-based composites with martensite phase. However, the uniformly distributed martensite phase and the volume fraction of the transformed martenstie phase should be controlled to further improve the mechanical properties of the materials.

Acknowledgements This work was supported by the Knowledge Innovation Program of the Chinese Academy of Sciences (Project number: KJCX2-SW-L05) and National Natural Science Foundation of China (Grant No. 50101012).

References

1. Louzguine, D. V., Kato, H., Inoue, A., High-strength Cu-based crystal-glassy composites with enhanced ductility, Appl. Phys. Lett., 2004, 84:1088－1090.
2. Hufnagel, T. C., El-Deiry, P., Vinci, R. P., Development of shear band structure during deformation of a $Zr_{51}Ti_5Cu_{20}Ni_8Al_{10}$ bulk metallic glass, Scr. Mater., 2000, 43: 1071－1077.
3. Bruck, H. A., Christman, T., Rosakis, A. J., Johnson, W. L., Quasi-static constitutive behavior of $Zr_{41.25}Ti_{15.75}Ni_{10}Cu_{12.5}Be_{22.5}$ bulk amorphous alloy, Scr. Metall. Mater., 1994, 30: 429－434.
4. Xing, L. Q., Li, Y., Ramesh, K. T., Enhanced plastic strain in Zr-based bulk amorphous alloys, Phys. Rev. B, 2001, 64: 180201-4.
5. Choi-Yim, H., Busch, R., Koster, U., Johnson, W. L., Synthesis and characterization of particles reinforced $Zr_{57}Nb_5Al_{10}Cu_{15.4}Ni_{12.6}$ bulk metallic glass composites, Acta Mater., 1999 47: 2455－2465.
6. Spaepen, F., A microscopic mechanism for steady state inhomogeneous flow in metallic glasses, Acta Metall., 1977, 25: 407－415.
7. Choi-Yim, H., Johnson, W. L., Bulk metallic glass matrix composites, Appl. Phys. Lett., 1997, 71: 3808－3810.
8. Bian, Z., Pan, M. X., Zhang, Y., Wang, W. H., Carbon-nanotube-reinforced $Zr_{52.5}Cu_{17.9}Ni_{14.6}Al_{10}Ti_5$ bulk metallic glass composites, Appl. Phys. Lett., 2002, 81: 4739－3741.
9. Ma, H., Xu, J., Ma, E., Mg-based bulk metallic glass composites with plasticity and high strength, Appl. Phys. Lett., 2003, 83: 2793－2795.
10. Kim, C. P., Busch, R., Johnson, W. L., Processing of carbon-fibre-reinforced $Zr_{41.2}Ti_{13.8}Cu_{12.5}Ni_{10}Be_{22.5}$ bulk metallic glass composites, Appl. Phys. Lett., 2001, 79: 1456－1458.
11. Leonhard, A., Xing, L. Q., Heilmaier, M., Eckert, J., Schultz, L., Effect of crystalline precipitations on the mechanical behavior of bulk glass forming Zr-based alloys, Nanostructured Mater., 1998, 10: 805－812.
12. Hays, C. C., Kim, C. P., Johnson, W. L., Microstructure controlled shear bands pattern formation and enhanced plasticity of bulk metallic glasses containing *in situ* formed ductile phase dendrite dispersion, Phys. Rev. Lett., 2000, 84: 2901－2906.
13. Kűhn, U., Eckert, J., Mattern, N., ZrNbCuNiAl bulk metallic glass matrix composites containing dendritic bcc phase precipitates, Appl. Phys. Lett., 2002, 80: 2478－2490.
14. Eckert, J., Kűhn, U., Mattern, N., Structural bulk metallic glasses with different length-scale of constituent phase, Intermetallics, 2002, 10: 1183－1190.
15. He, G., Eckert, J., Loser, W., Schultz, L., Novel Ti-base nanostructure-dendrite composite with enhanced plasticity, Nature Mater., 2003, 2: 33－38.
16. Yokoyanma, Y., Kobayashi, A., Fukaura, K., Inoue, A., Oxygen embrittlement and effect of addition of Ni element in a bulk amorphous Zr-Cu-Al alloy, Mater. Trans. JIM, 2002, 43: 571－574.
17. Nicholls, A. W., Harris, I. R., Indentification of phase resulting from the transformation of the intermetallic phase ZrCu, J. Mater. Sci. Lett., 1986, 5: 217－220.
18. Carvalho, E. M., Harris, I. R., Constitutional and structural studies of the intermetallic phase, ZrCu, J. Mater. Sci., 1980, 15: 1224－1230.
19. Seo, J. W., Schryvers, D., TEM investigation of the microstructure and defects of CuZr martensite (I): Morphology and twin systems, Acta Mater, 1998, 46: 1165－1175.
20. Seo, J. W., Schryvers, D., TEM investigation of the microstructure and defects of CuZr martensite (II): Planar defects, Acta Mater.,1998, 46: 1177－1183.
21. Wang, H. R., Ye, Y. F., Shi, Z. Q., Crystallization process in amorphous $Zr_{54}Cu_{46}$ alloy, J. Non-cryst. Solid, 2002, 36: 311.

(Received June 28, 2005; accepted August 9, 2005)